XI International Conference on Computational Plasticity. Fundamentals and Applications
COMPLAS XI
E. Oñate, D.R.J. Owen, D. Peric and B. Suárez (Eds)

MULTI-SCALE MODELLING FOR FERRITE-PEARLITE COMPOSITE STEEL

IKUMU WATANABE*, DAIGO SETOYAMA† AND NORITOSHI IWATA†

*National Institute for Materials Science (NIMS)
Sengen 1-2-1, Tsukuba, Ibaraki, 305-0047 Japan
e-mail: WATANABE.Ikumu@nims.go.jp, www.nims.go.jp/

†TOYOTA Central R&D Labs., Inc. (TCRDL)
Yokomichi 41-1, Nagakute, Aichi 480-1192 JAPAN

Key words: Microstructures, Multiscale Modeling, Finite Element Method

Abstract. The multiscale mechanical behaviors of Ferrite-Pearlite steel were predicted using Numerical Material Testing (NMT) based on the finite element method. The microstructure of Ferrite-Pearlite steel is regarded as a two-component aggregate of Ferrite crystal grains and Pearlite colonies. In the NMT, the macroscopic stress-strain curve and the deformation state of the microstructure were examined by means of a two-scale finite element analysis method based on the framework of the mathematical homogenization theory. For the NMT of Ferrite-Pearlite steel, constitutive models for Ferrite crystal grains and Pealite colonies were prepared to describe the anisotropic mechanical behavior at the micro-scale.

1 INTRODUCTION

The macroscopic material behavior is governed by the microstructure. The numerical homogenization approach was to evaluate the macroscopic material behavior from its microscopic information with a computational method, namely the finite element method. The feature of this methodology is that the morphology of the microstructure can be explicitly modeled with finite elements. Then the interaction between each component can be mechanically taken into consideration. In addition, the microscopic model undergoes the numerical examination under idealized macroscopic and microscopic states over and over again, which is almost impossible when carrying out actual experiments. In this study, the computational framework used to examine the material behavior is called *Numerical Material Testing* (NMT).

The key element to the success of such a numerical homogenization approach is to be able to describe the microscopic mechanism realistically in the form of a computational

model. Special attention has to be paid to constitutive models for each component of the microstructure in order to describe the microscopic material behavior. It should be noted that the microscopic material behavior is anisotropic even if the macroscopic material behavior is isotropic, making the standard constitutive models for macro-scale problem completely unsuitable to the microscopic components in general. The single crystal plasticity model is a well-known microscopic constitutive model for a metallic material, which expresses the crystallographically-defined plastic anisotropy.

Turning to the application of the computational approach based on the continuum mechanics into steel, various studies have been made on the numerical evaluation of the mechanical behavior because of the practical importance of steel as a structural material. General carbon steels are characterized with the precipitation of Cementite, which is an iron carbide, in various forms. A typical microstructure of Ferrite-Pearlite steel is depicted in Figure1, which is composed of several Ferrite crystal grains and Pearlite blocks. And a Pearlite block contains some Pearlite colonies characterized by the lamellar structures of Ferrite and Cementite phases. Such hierarchical heterogeneity is the dominant factor of the strength and the deformation characteristic.

In this study, we apply the framework of an NMT to evaluate and model the hierarchical mechanical behavior of Ferrite-Pearlite steel. Both anisotropic linear elasticity and single crystal plasticity models can be employed to describe the mechanical behavior of Ferrite crystal grains. However, the anisotropic constitutive model for Pearlite colonies has yet to be proposed. The constitutive model is newly formulated in reference to the results of the NMT for the microscopic lamellar structures composed of Ferrite and Cementite phases: that is, the NMT is carried out to produce mechanical behavior for the formulation of microscopic constitutive equations which can be substituted for the constitutive theory. In this sense, it is possible to approach the evaluation of mechanical behavior using physical computations as first principle calculations although the applicability of this approach is limited to elastic regions, given the limits we have.

2 HOMOGENIZATION METHOD AND CONSTITUTIVE MODEL FOR FERRITE CRYSTAL

2.1 Homogenization approach based on finite element method

In the two-scale finite element analysis method [1], a representative volume element (RVE) of the microstructure is discretized with finite elements and the microscopic boundary value problem (BVP) is simultaneously solved with the macroscopic BVP in the two-scale BVP. We here reduce the macroscopic BVP to a point-wise stress-strain relationship. Then the two-scale BVP turns into a problem to evaluate the material behavior of a numerical specimen represented as a microscopic finite element model under the control of the macroscopic stress or strain, i.e. this framework is regarded as *Numerical Material Testing* (NMT) based on the finite element method [2].

With this framework, we can evaluate both the macroscopic material response and

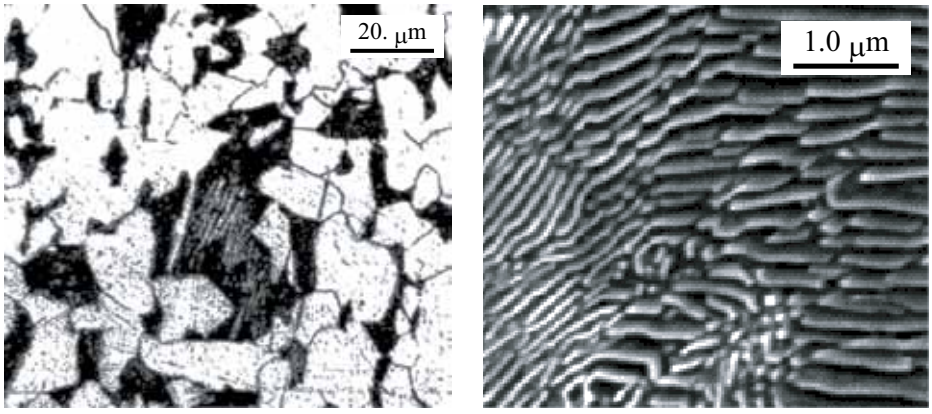

(a) Ferrite-Pearlite steel (b) Pearlite block

Figure 1: Microstructure of Ferrite-Pearlite steel. The Microstructure of Ferrite-Pearlite steel is composed of several Ferrite crystal grains and Pearlite blocks. Pearlite block contains some Pearlite colonies characterized with the lamellar structure of Ferrite and Cementite phases.

the deformation state of a microstructure. By conducting a series of numerical material tests, the macroscopic material response of the microstructure is examined in detail. In this study, we employ the computational approach to develop an anisotropic constitutive model depending on the morphology of the intended microstructure and identify the material constants of the constitutive model.

2.2 Elastic-plastic constitutive model for Ferrite single crystal

An anisotropic linear elasticity and a single crystal plasticity are introduced to capture the anisotropic mechanical behavior of a single crystal.

Here, we use the single crystal plasticity based on the representative characteristic length [3]. In this constitutive model, the critical resolved shear stress (CRSS) is characterized with the representative characteristic length, which in turn represents the dominant strengthening mechanics. In addition, the yield-point elongation and the hardening behavior can be described with the evolution of the dislocation density.

3 ELASTIC-PLASTIC CONSTITUTIVE MODEL FOR PEARLITE COLONY

3.1 Finite element model for Pearlite colony

The finite element model of the Pearlite colony is defined as shown in Figure2, where the white elements indicate the Ferrite phase and the others are Cementite phases. It is assumed that the Ferrite and Cementite lamellar structures are completely parallel with each other, the boundary between them does not slip, and this finite element model satisfies the geometrical periodicity boundary condition. Also, the normal vector, $\boldsymbol{m}_0$, of the lamella is set as heading in the direction of Y_3 at the initial configuration for the

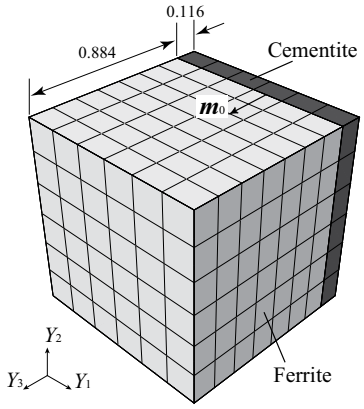

Figure 2: Finite element model of Pearlite colony. The white and shaded areas indicate the Ferrite and Cementite phases, respectively. The normal vector of the lamella indicates $\boldsymbol{m}_0$ at the initial state.

formulation of the constitutive model. Here we employ the crystallographic orientation relationships of Bagaryatskii [4] as below:

$$\begin{cases} (001)_{\text{Cementite}} \ // \ (211)_{\text{Ferrite}} \\ [100]_{\text{Cementite}} \ // \ [0-11]_{\text{Ferrite}} \\ [010]_{\text{Cementite}} \ // \ [-111]_{\text{Ferrite}} \end{cases} \tag{1}$$

In addition, the mechanical character of the Cementite phase is considered as an elastic material, whereas this does not seem to be true in the finite strain range as mentioned later.

3.2 Numerical Material Tests for Pearlite colony

The macroscopic elastic-plastic material behavior was investigated with an NMT for the microscopic finite element model of the Pearlite colony.

3.2.1 Elasticity

The components of the fourth order elastic tensor were estimated with finite element analyses of the RVE (Figure2). Before that, however, the elastic constants of both the Ferrite and Cementite phases must be prepared for computation. For the Ferrite phase, the values were taken from the experimental database. The metastability of Cementite, however, makes it extremely difficult to estimate the elasticity of Cementite phase. The first-principles calculations in this study were performed by the projector augmented wave method [5, 6] as implemented in the Vienna *ab-initio* simulation package (VASP) [7, 8]. The elastic constants estimated from the calculation are presented as below, where the

Table 1: Components of fourth order elastic tensor for Pearlite colony.

Component	$\hat{\mathbb{C}}^{e}_{1111}$	$\hat{\mathbb{C}}^{e}_{2222}$	$\hat{\mathbb{C}}^{e}_{3333}$	$\hat{\mathbb{C}}^{e}_{1122}$	$\hat{\mathbb{C}}^{e}_{2233}$	$\hat{\mathbb{C}}^{e}_{1133}$	$\hat{\mathbb{C}}^{e}_{1212}$	$\hat{\mathbb{C}}^{e}_{1313}$	$\hat{\mathbb{C}}^{e}_{2323}$
[GPa]	302.	313.	292.	98.	100.	115.	69.	94.	74.
Component	$\hat{\mathbb{C}}^{e}_{1112}$	$\hat{\mathbb{C}}^{e}_{1113}$	$\hat{\mathbb{C}}^{e}_{1123}$	$\hat{\mathbb{C}}^{e}_{2212}$	$\hat{\mathbb{C}}^{e}_{2213}$	$\hat{\mathbb{C}}^{e}_{2223}$	$\hat{\mathbb{C}}^{e}_{3312}$	$\hat{\mathbb{C}}^{e}_{3313}$	$\hat{\mathbb{C}}^{e}_{3323}$
[GPa]	0.	0.	-26	0.	-26	1.	0.	0.	27.

Component	$\hat{\mathbb{C}}^{e}_{1213}$	$\hat{\mathbb{C}}^{e}_{1223}$	$\hat{\mathbb{C}}^{e}_{1323}$
[GPa]	0.	0.	0.

anisotropy is orthotropic in type.

$$\begin{array}{lll} \hat{\mathbb{C}}^{e(Fe_3C)}_{1111} = 397.0\text{GPa} & \hat{\mathbb{C}}^{e(Fe_3C)}_{2222} = 364.0\text{GPa} & \hat{\mathbb{C}}^{e(Fe_3C)}_{3333} = 317.\text{GPa} \\ \hat{\mathbb{C}}^{e(Fe_3C)}_{1122} = 168.\text{GPa} & \hat{\mathbb{C}}^{e(Fe_3C)}_{2233} = 183.3\text{GPa} & \hat{\mathbb{C}}^{e(Fe_3C)}_{1133} = 154.\text{GPa} \\ \hat{\mathbb{C}}^{e(Fe_3C)}_{1212} = 66.\text{GPa} & \hat{\mathbb{C}}^{e(Fe_3C)}_{1313} = 138.\text{GPa} & \hat{\mathbb{C}}^{e(Fe_3C)}_{2323} = 142.\text{GPa} \end{array} \tag{2}$$

Using the finite element model presented in Figure2 and the elastic constants, the components of the elastic tensor of Pearlite colony were numerically evaluated, with the macroscopic deformation modes corresponding to each strain component imposed on the finite element model of the microstructure. The resulting values are give in Table1, where the anisotropy is described with twenty-one independent elastic constants.

3.2.2 Plasticity

After determining the elastic material behavior of the Pearlite colony, the next step was to evaluate its plasticity with an NMT based on the finite element method. Here it is assumed that the Cementite phase is elastic. Also, the elastic-plastic material behavior of the Ferrite phase was characterized with the constitutive model explained in Section 2.2. The material constants of the plasticity of the Ferrite phase were found after trial and error by comparing between a result of an experimental axial tensile test for a Ferrite single-phase steel and the macroscopic stress-strain curve of the corresponding NMT. Considering the rotational symmetry of the lamellar structure for the third coordinate axis, five macroscopic deformation modes, i.e. the five components of macroscopic displacement gradient listed below, were respectively imposed on the finite element model of the microstructure of Pearlite colony (Figure2) until there was sufficient large strain to describe the macroscopic plastic behavior:

$$\tilde{H}_{11}, \quad \tilde{H}_{12}, \quad \tilde{H}_{13}, \quad \tilde{H}_{31}, \quad \tilde{H}_{33}, \tag{3}$$

which are two types of uniaxial deformation mode and three types of simple shear deformation mode.

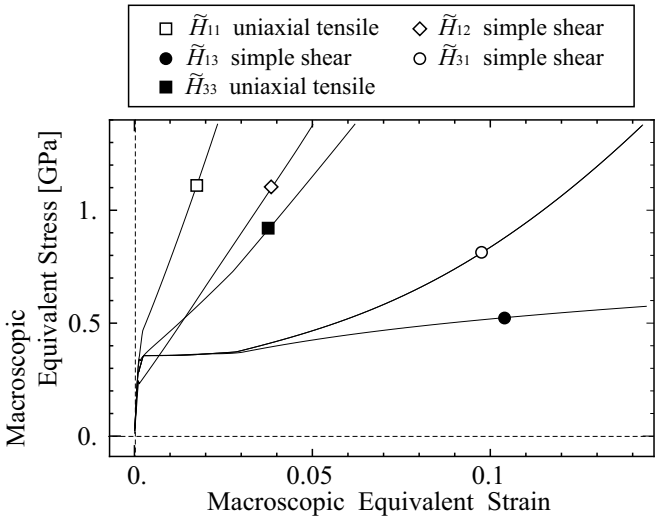

Figure 3: Macroscopic stress-strain curves of Pearlite colony.

The resulting macroscopic, or homogenized, equivalent stress-strain curves are illustrated in Figure3, where the equivalent stress is the Mises stress and the equivalent strain is defined with Henky strain $\boldsymbol{\epsilon} = \frac{1}{2}\ln\left[\boldsymbol{F}\boldsymbol{F}^{\mathrm{T}}\right]$ as

$$\epsilon^* := \sqrt{\frac{2}{3}\mathrm{dev}\left[\boldsymbol{\epsilon}\right] : \mathrm{dev}\left[\boldsymbol{\epsilon}\right]}. \tag{4}$$

As it can be seen, the results clearly indicate strong anisotropic plastic behavior, which is extremely stiff after yielding except in the case of the simple shear deformation modes $\tilde{H}_{13}$ and $\tilde{H}_{31}$. The response of $\tilde{H}_{13}$, the interlamellar shear deformation mode, is particularly close to the material behavior of the Ferrite phase.

With regard to the microscopic investigation, three representative deformation states and stress values at a macroscopic equivalent strain of 10 % are depicted in Figure4 with the equivalent stress values of each phases. It needs to be pointed out that the stress values of the Cementite phase are unrealistically high in these results except for the interlamellar shear deformation mode. It is quite likely that such a high stress state induces some dissipation mechanics, e.g. in the plastic behavior of the Cementite phase or debonding at the boundary between the Ferrite and Cementite phases. Although some studies have been carried out with the aim of observing such microscopic material behavior, the deformation mechanism of the Cementite phase at finite strain is still controversial. Regardless of the cause of the dissipation behavior, the plastic deformation of the Ferrite phase appears to be released from the constraint and also the macroscopic yielding stands out on the macroscopic, or homogenized, stress-strain curve of Pearlite colony.

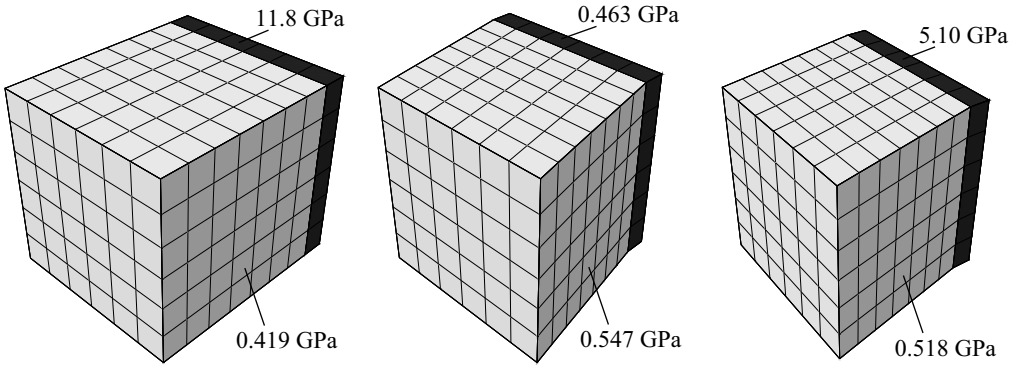

(a) $\tilde{H}_{33}$ (uniaxial tensile) (b) $\tilde{H}_{13}$ (simple shear) (c) $\tilde{H}_{31}$ (simple shear)

Figure 4: Microscopic deformation state of Pearlite colony. The stress states are homogeneous in each phase and the equivalent stress values are written in the Figure.

3.3 Plastic constitutive model for Pearlite colony

Based on the characterization of the anisotropic material behavior using the NMT, we propose the anisotropic plastic constitutive model for the Pearlite colony. In this study, the plastic behavior of the Pearlite colony is defined as two-stage yielding behavior; interlamellar shear yielding and the yielding of overall microstructure. That is, the plastic constitutive model for the Pearlite colony is described with two yield functions consisted of an anisotropic interlamellar shear plasticity and a standard isotropic metal plasticity. For the Kirchhoff stress $\boldsymbol{\tau}$ and the plastic internal variables $\zeta^{(\alpha)}$ ($\alpha = 1, 2$), the two yield functions are defined at current configuration as below:

$$\psi^{(1)} := |\boldsymbol{s} \cdot (\boldsymbol{\tau}\boldsymbol{m})| - \left(\tau_{\mathrm{Y}}^{(1)} + h_{11}\zeta^{(1)} + h_{12}\zeta^{(2)}\right) \leq 0 \tag{5}$$

$$\psi^{(2)} := \sqrt{\frac{3}{2}\mathrm{dev}[\boldsymbol{\tau}] : \mathrm{dev}[\boldsymbol{\tau}]} - \left(\tau_{\mathrm{Y}}^{(2)} + h_{21}\zeta^{(1)} + h_{22}\zeta^{(2)}\right) \leq 0 \tag{6}$$

where $\tau_{\mathrm{Y}}^{(\alpha)}$ is the initial yield stress for the α-th yield function ($\alpha = 1$ or 2) and $h_{\alpha\beta}$ ($\alpha, \beta =$ 1 or 2) is the hardening coefficient containing cross-hardening. The first yield function $\psi^{(1)}$ represents the slip behavior on the lamellar structure. The slip direction vector $\boldsymbol{s}$ and the normal vector $\boldsymbol{m}$ are pushed forward from the intermediate configuration with the elastic deformation gradient $\boldsymbol{F}^{\mathrm{e}}$ as

$$\boldsymbol{s} = \boldsymbol{F}^{\mathrm{e}}\boldsymbol{s}_0, \quad \boldsymbol{m} = \boldsymbol{F}^{\mathrm{e}-\mathrm{T}}\boldsymbol{m}_0, \tag{7}$$

where $\boldsymbol{s}_0$ and $\boldsymbol{m}_0$ are respectively the slip direction vector and the normal vector of the lamella at the intermediate configuration. With equation (7), the yield functions at the

intermediate configuration are given as below:

$$\psi^{(1)} := \left|\hat{\boldsymbol{T}} : (\boldsymbol{s}_0 \otimes \boldsymbol{m}_0)\right| - \left(\tau_{\mathrm{Y}}^{(1)} + h_{11}\zeta^{(1)} + h_{12}\zeta^{(2)}\right) \leq 0 \tag{8}$$

$$\psi^{(2)} := \sqrt{\frac{3}{2}\mathrm{dev}[\hat{\boldsymbol{T}}] : \left(\mathrm{dev}[\hat{\boldsymbol{T}}]\right)^{\mathrm{T}}} - \left(\tau_{\mathrm{Y}}^{(2)} + h_{21}\zeta^{(1)} + h_{22}\zeta^{(2)}\right) \leq 0 \tag{9}$$

The slip direction vector $\boldsymbol{s}_0$ is determined as the unit vector which indicates the direction of the innerlamellar component of the traction force vector $\hat{\boldsymbol{T}}\boldsymbol{m}_0$ on the lamella, i.e. it is defined with the normal vector $\boldsymbol{m}_0$ and the stress state $\hat{\boldsymbol{T}}$ as below:

$$\boldsymbol{s}_0 := \frac{\boldsymbol{t}}{\sqrt{\boldsymbol{t}\cdot\boldsymbol{t}}}, \qquad \boldsymbol{t} := \hat{\boldsymbol{T}}\boldsymbol{m}_0 - \left\{\boldsymbol{m}_0 \cdot \left(\hat{\boldsymbol{T}}\boldsymbol{m}_0\right)\right\}\boldsymbol{m}_0 \tag{10}$$

In equations (8) and (9), only h_{22} is defined as a non-linear function of $\zeta^{(1)}$ to express the non-linear hardening behavior:

$$h_{22} := \left(h_{22}^0 - h_{22}^\infty\right)\exp\left[-p\zeta^{(2)}\right] + h_{22}^\infty, \tag{11}$$

where p is a sensitivity of the exponential function, h_{22}^0 is the initial value of h_{22} and h_{22}^∞ is the corresponding convergent value. In this study, we are not concerned with the strengthening effect of lamellar spacing, but it is possible to introduce the effect on the material constants of the initial strength and the hardening behavior.

Finally, the proposed constitutive model was examined by making a comparison between its response and the results of the NMT of the Pearlite colony. The equivalent stress-strain curves are evaluated for three deformation modes corresponding to the components of the displacement gradient, H_{11}, H_{13} and H_{31}, where it is assumed that the vector $\boldsymbol{m}_0$ is directed to the coordinate axis direction Y_3 in the same way as the finite element model in Figure2. Here the plastic behavior of the interlamellar shear deformation mode is determined from NMT, and the constants of isotropic hardening were found by trial and error as they were for the Ferrite phase. The results are shown in Figure5.

4 NUMERICAL ANALYSIS FOR FERRITE-PEARLITE STEEL

The NMT based on finite element method was performed to predict the mechanical behavior of Ferrite-Pearlite steel with the constitutive models discussed in Section 2 and 3, and the computational results were compared with the experimental results.

4.1 Setting of finite element model of microstructure

We set the finite element models of the microstructure for Ferrite-Pearlite steel to carry out the following NMT.

The basic finite element model given in Figure6 is assumed to satisfy the geometrical periodicity condition and is composed of fifty-four blocks. In this finite element model, each block has an idealized geometry of truncated octahedrons and is discretized by eighty

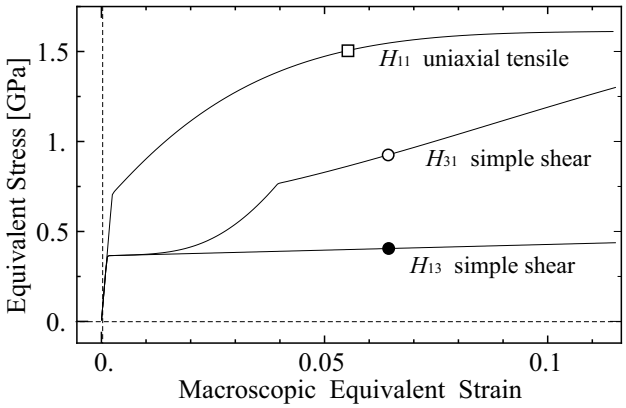

Figure 5: Stress-strain curves of constitutive model of Pearlite colony. The vector $\boldsymbol{m}_0$ is set up as an unit vector directed to third coordinate axis.

standard isoparametric hexahedron finite elements. In addition, each block is recognized as either Ferrite or Pearlite. The properties of the blocks are randomly arranged in accordance with the volume fraction of the Ferrite-Pearlite steel under consideration, where the discretely-distributed microstructure of Ferrite-Pearlite steel is supposed as Figure1(a); the finite element model shown in Figure6 is made of 33 percent Pearlite. If the property of a block is Ferrite, the block is recognized as a single grain. If it is Pearlite, the block is equally divided into eight colonies as illustrated in Figure6. That is, Pearlite always exists as an aggregate composed of some Pearlite colonies. Anisotropic elastic-plastic constitutive models for Ferrite single crystals and Pearlite colonies, which are presented in Section 2 and 3, are employed for the corresponding components. As mentioned before, some material constants of plasticity were determined to reproduce the stress-strain curves in experimental axial tensile tests as the results of the homogenization analyses. The orientations of each Ferrite crystal grain and Pearlite colony, i.e. the crystallographic orientations and the direction of the normal vector of the lamella, are provided in a random fashion.

4.2 Numerical results and validation

First, we investigate the elastic constants of Ferrite single-phase steel (Pearlite volume fraction 0 percent) and full Pearlite steel (Pearlite volume fraction 100 percent) with an NMT for the microstructure shown in Figure6, which is the same as the NMT used for the Pearlite colony. The almost isotropic material behaviors are evaluated in this computations. The results were acceptable values of the Young modulus and Poisson's ratio for each steel, as estimated as below:

$$\begin{aligned} E^{(\text{Ferrite})} &\simeq 200.\ \text{GPa} \qquad & \nu^{(\text{Ferrite})} &\simeq 0.296 \\ E^{(\text{Pearlite})} &\simeq 216.\ \text{GPa} \qquad & \nu^{(\text{Pearlite})} &\simeq 0.288 \end{aligned} \tag{12}$$

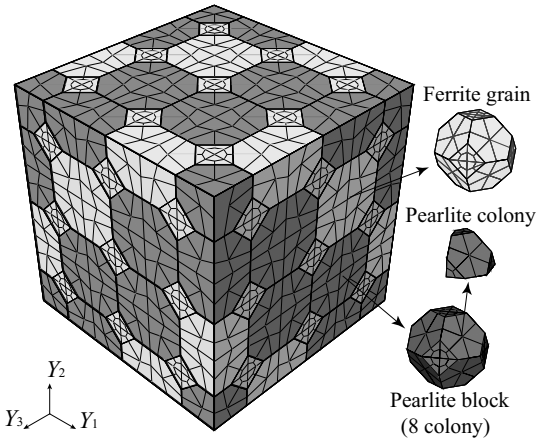

Figure 6: Finite element model of microstructure of Ferrite-Pearlite steel. The finite element model is composed of 54 blocks. Each block has an idealized geometry of a truncated octahedron and is recognized as a Ferrite crystal grain or a Pearlite block equally divided into eight colonies.

Obviously, the elasticity of Ferrite-Pearlite steel takes a value intermediate between these.

Next, we performed a series of numerical experiments in which the volume fraction of Ferrite/Pearlite was changed. Macroscopic uniaxial tensile deformation was imposed to the finite element model of Ferrite-Pearlite microstructure in the corresponding Y_1 direction, as illustrated in Figure6. The resulting macroscopic stress-strain curves are almost isotropic because Ferrite and Pearlite blocks are randomly arranged in the finite element model of the microstructures. The macroscopic, or homogenized, axial stress-strain curves of five cases are presented in Figure7, where the experimental results of three cases, Pearlite volume fraction 0 percent, 38 percent and 100 percent, are illustrated together by the dashed lines. Here we prepare a tensile test specimen of Ferrite-Pearlite steel which consists of almost the same scale of lamellar spacing with the corresponding specimen of full Pearlite steel to cut off a strengthening effect of the lamellar spacing.

The numerical results for Pearlite with a volume fraction of 0 percent and 100 percent is obiously similar since the material constants of the results of the NMTs reproduce the experimental results. Furthermore the experimental stress-strain curve of the Ferrite-Pearlite steel with a volume fraction of 38 percent is close to the numerical result with a 33 percent volume fraction. Therefore it is concluded that this NMT successfully predicted macroscopic mechanical behavior.

For the composite case (Pearlite volume fraction 33 percent, i.e. the finite element model Figure6), the distributions of equivalent stress and maximum principal strain are depicted in Figure8 at the point where the macroscopic axial strain is 15 percent. In this figure, the stress states are significantly different between Ferrite grains and Pearlite blocks. Compared to the arrangement of Ferrite grains and Pearlite blocks in Figure6, the Ferrite grains underwent more plastic deformation than the Pearlite blocks due to the

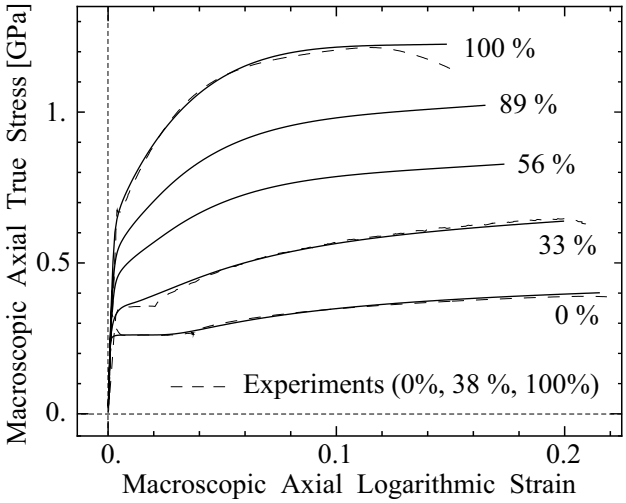

Figure 7: Macroscopic axial stress-strain curves of Ferrite-Pearlite steel. The solid and the dash lines indicate numerical and experimental results respectively.

higher yield strength of the Pearlite blocks.

5 CONCLUSIONS

We have predicted multiscale mechanical behavior of Ferrite-Pearlite steel with the hierarchical Numerical Material Testing using a deductive approach. A first principle calculation was performed to estimate the components of fourth order elastic tensor of the Cementite phase. With the elastic tensor, an NMT based on the finite element analysis was conducted to evaluate the anisotropic mechanical behavior of a Pearlite colony. Based on the resultant homogenized mechanical behavior of the Pearlite colony, an anisotropic plastic constitutive model for Pearlite colonies proposed to enable the NMT for Ferrite-Pearlite steel to be carried out. Finally, both the macroscopic and microscopic mechanical behavior of Ferrite-Pearlite steel was predicted with the NMT. We were thus able to demonstrate that this numerical approach provides acceptable results at both the macro- and micro-scale.

REFERENCES

[1] Terada K, Saiki I, Matsui K, Yamakawa Y. Two-scale kinematics and linearization for simultaneous two-scale analysis of periodic heterogeneous solids at finite strain. *Comput Meth Appl Mech Eng* (2003) **192** 3531–3563.

[2] Watanabe I, Terada K. A method of predicting macroscopic yield strength of polycrystalline metals subjected to plastic forming by micro-macro de-coupling scheme. *Int J Mech Sci* (2010) **52** 343–355.

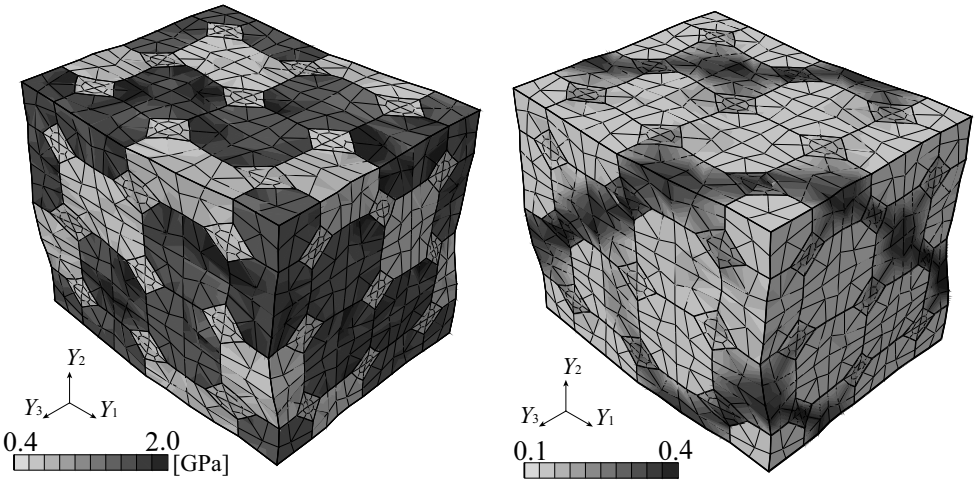

(a) Equivalent stress (b) Maximum principal strain

Figure 8: Microscopic stress and strain distributions for Ferrite-Pearlite steel. These figures show the results of the case of Pearlite volume fraction 33 % at a point of macroscopic axial strain 15 % on macroscopic axial stress-strain curve of Figure7.

[3] Watanabe I, Setoyama D, Iwata N, Nakanishi K. Characterization of yielding behavior of polycrystalline metals with single crystal plasticity based on representative characteristic length. *Int J Plasticity* (2010) **26** 570–585.

[4] Bagaryatskii YA. Possible mechanism of martensite decomposition. *Dokl Acad Nauk SSSR* (1950) **73** 1161–1164,.

[5] Blöchl PE. Projector augmented-wave method. *Phys Rev B* (1994) **50** 17953–17979.

[6] Kresse G, Joubert D. From ultrasoft pseudopotentials to the projector augmented-wave method. *Phys Rev B* (1999) **59** 1758–1775.

[7] Kresse G, Furthmuller J. Efficiency of ab-initio total energy calculations for metals and semiconductors using a plane-wave basis set. *Comput Mater Sci* (1996) **6** 15–50.

[8] Kresse G, Furthmuller J. Efficient iterative schemes for ab initio total-energy calculations using a plane-wave basis set. *Phys Rev B* (1996) **50** 11169–11186.